

# Spin lifetimes and strain-controlled spin precession of drifting electrons in zinc blende type semiconductors

M. Beck, C. Metzner, S. Malzer, and G. H. Döhler

*Institut für Technische Physik I, Universität Erlangen-Nürnberg, Erlangen, Germany*

(Dated: November 21, 2018)

We study the transport of spin polarized electrons in n-GaAs using spatially resolved continuous wave Faraday rotation. From the measured steady state distribution, we determine spin relaxation times under drift conditions and, in the presence of strain, the induced spin splitting from the observed spin precession. Controlled variation of strain along [110] allows us to deduce the deformation potential causing this effect, while strain along [100] has no effect. The electric field dependence of the spin lifetime is explained quantitatively in terms of an increase of the electron temperature.

Sufficiently long spin lifetimes and the possibility to manipulate the spin orientation are required for the development of spintronics devices [1]. Electron spin lifetimes  $\tau_s$  in semiconductors have been measured by means of the Hanle effect (depolarization of photoluminescence in a magnetic field) [2], time resolved photoluminescence [3], and time resolved measurements of magneto-optical effects (Faraday / Kerr rotation) [4], which are suitable to measure  $\tau_s$  in the absence of holes. Although future spintronics applications are likely to depend on spin *transport*, very little attention has been paid to the influence of an electric drift field  $F$  on  $\tau_s$ . While the possibility to transport the electron spin over substantial distances in fields up to  $F = 100$  V/cm has been demonstrated several years ago [5], first measurements of  $\tau_s$  in this field range have only been reported recently [7]. Under the influence of strain, spin precession of the drifting electrons [5, 6, 8] has been observed and even the possibility to generate spin polarized currents without magnetic materials or optical excitation has been demonstrated [7]. However, no theoretical interpretation of the observed spin lifetimes and no quantitative analysis of the influence of strain on the observed spin splitting has been given.

In this Letter, we present a method to study the lateral spin transport in thin films of n-doped GaAs under steady state conditions, similar to the experiments reported recently in [8], but with the possibility to determine spin lifetimes and to quantify the influence of strain. By the absorption of circularly polarized light we locally generate a steady-state electron spin polarization and determine the spin drift length  $L_s$  from the spatial decay of spin polarization along the drift direction, which results from the combined process of electron diffusion, drift and spin relaxation. As this signal can be traced over several 100  $\mu\text{m}$  while the signal varies by up to three orders of magnitude, this cw method allows for accurate measurements of the electric field, doping density and temperature dependence of  $L_s$ . Knowing the drift velocity  $v_{\text{dr}}$ , the spin relaxation time  $\tau_s$  can be determined from  $L_s$ . In the presence of strain, we observe spin precession in addition to the spatial decay. As realistic theoretical pre-

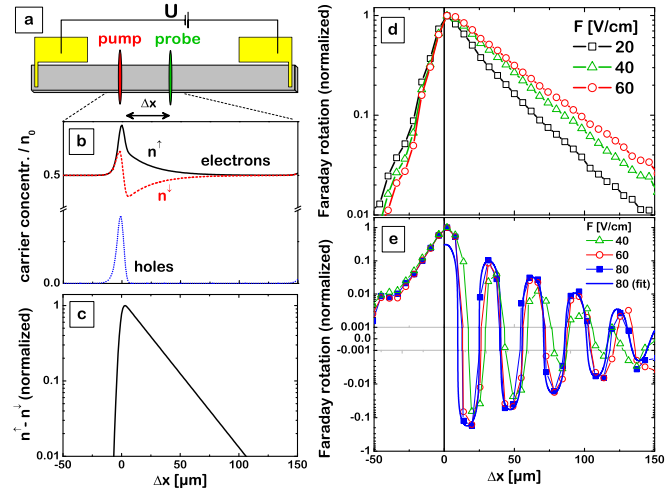


FIG. 1: (a) Principle of the experiment; (b) example of an expected spatial distribution of holes and spin up and spin down electrons (divided by the equilibrium electron concentration  $n_0$ ); (c) expected normalized electron spin polarization; (d),(e): examples of the measured spatially resolved Faraday rotation in an unstrained sample (d) and in a strained (here: unknown, uncontrolled strain) sample (e), plotted on two logarithmic scales connected with a linearly scaled region in order to visualize the exponential decay. The fit function to the data for  $F = 80$  V/cm is given by  $A \exp[(\Delta x - x_0)/\Lambda_d] \cos[2\pi(\Delta x - x_0)/\Lambda_p]$ .

dictions of the spin transport in an electric field were not available we have also performed such calculations. We find excellent agreement between experiment and theory both in the unstrained and the strained case and can deduce an experimental value for the band structure parameter controlling the strain-induced spin precession.

The principle of our measurement is illustrated in Fig. 1(a–c). The samples, grown by molecular beam epitaxy, are  $1 \times 0.1 \text{ mm}^2$  bars (oriented along [110],  $[\bar{1}\bar{1}0]$ , [100],  $[010]$ ) of silicon (n-type) doped (doping densities  $N_D = 10^{15} \text{ cm}^{-3} \dots 6 \times 10^{16} \text{ cm}^{-3}$ ) layers of GaAs (typically 1  $\mu\text{m}$  thick; up to 5  $\mu\text{m}$  for low  $N_D$ ) in between two undoped  $\text{Al}_{0.3}\text{Ga}_{0.7}\text{As}$  barriers (to avoid surface effects), lifted from the substrate by epitaxial lift-off and

attached to glass by van-der-Waals bonding. Circularly polarized light from a cw laser diode (“pump”; typically 1.52 eV, 1 mW) excites spin polarized electron hole pairs in the GaAs layer which diffuse and, in the case of a finite electric field, drift laterally within the layer. The Faraday rotation of linearly polarized light from a second cw laser diode (“probe”; typically 1.512 eV, 0.2 mW) is used to measure the electron spin polarization. After passing through the sample, located in a liquid helium flow cryostat (temperature  $T_L \approx 5$  K for all reported measurements), the probe light is split by a Wollaston prism into two components, linearly polarized  $\pm 45^\circ$  with respect to the initial polarization. The intensity difference of these components is detected using lock-in technique at the sum of the modulation frequencies of the pump and probe laser diodes. The difference between the signals obtained for left and right circular excitation reflects the Faraday rotation induced by the spin polarized electrons. A stepper motor varies the pump-probe distance along the direction of  $F$ . The used edge emitting quantum well lasers give line-shaped spots on the sample ( $\approx 200 \times 5 \mu\text{m}^2$ ). Hence, since the layer thickness is much smaller than the transport distances under consideration and the excitation is approximately homogeneous across the sample, the transport can be treated as one-dimensional, which is essential for the straightforward determination of  $\tau_s$ . Fig. 1(b) shows a simulation of the carrier concentrations along the drift direction for typical parameters. Since the hole spin relaxes within picoseconds, the recombination ( $\tau_{\text{rec}} \approx 1$  ns) with electrons leaves behind a net electron spin polarization decaying exponentially on the way towards the positive contact [Fig. 1(b,c)]. In unstrained samples, we observe this exponential decay along the drift direction [Fig. 1(d)]. While the “downstream” spin diffusion length  $\Lambda_d$  along the drift direction increases with increasing field, the “upstream” diffusion in the opposite direction, characterized by  $\Lambda_u$  reduces. In strained samples, we additionally observe spin precession along the transport direction [Fig. 1(e)], similar to the spatio-temporally resolved results reported in [5, 6, 7] or the images of two-dimensional transport in [8]. Since, as will be shown below, the spin splitting depends linearly on the wave vector, the precession length  $\Lambda_p$  practically does not change with the electric field. The thick solid line is a fit to the results for  $F = 80$  V/cm with the function  $A \exp[-(\Delta x - x_0)/\Lambda_d] \cos[2\pi(\Delta x - x_0)/\Lambda_p]$ .

To quantify the influence of strain, we have carefully fabricated strain-free samples to which we have then applied strain in a systematic manner. Unintentional uniaxial strain during cool-down can be avoided by not attaching the glass substrate to any other material. Biaxial in-plane strain should be small, due to the similar thermal expansion coefficients of glass and GaAs. We control the strain by bending the glass substrate. Fig. 2 shows schematically our fixture used to vary the strain by turning the screws. The magnitude of strain is deter-

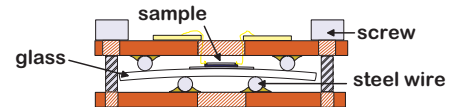


FIG. 2: Setup used to control the sample strain. Tightening the screws essentially stretches the sample in the direction perpendicular to the wires (uniaxial strain).

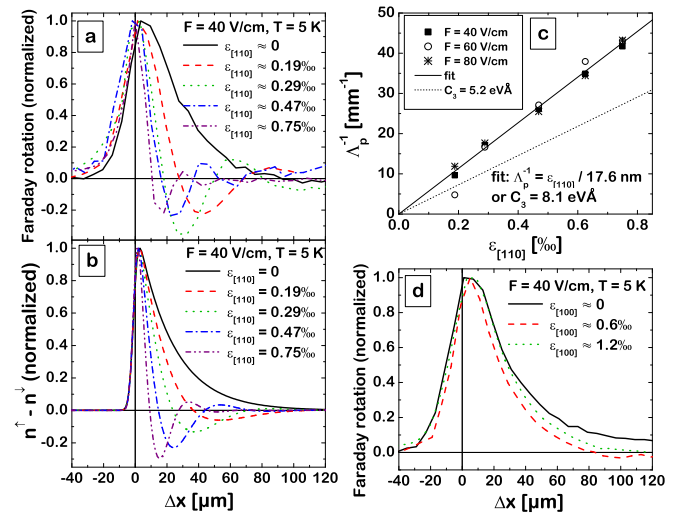


FIG. 3: Spin transport at  $F = 40$  V/cm and  $N_D = 1.4 \times 10^{16} \text{ cm}^{-3}$  in strained samples. (a) measured Faraday rotation for drift along  $[1\bar{1}0]$  and strain along  $[110]$ ; (b) calculated spin polarization with the parameters of (a) (using  $C_3 = 5.2 \text{ eV}\text{\AA}$ ); (c)  $\Lambda_p^{-1}$  versus strain  $\epsilon_{[110]}$ , linear fit corresponding to  $C_3 = 8.1 \text{ eV}\text{\AA}$ , and expected result for  $C_3 = 5.2 \text{ eV}\text{\AA}$  (dotted line); (d) measured Faraday rotation for drift and strain along  $[100]$ .

mined from the focal length of light reflected from the concave side of the glass. The measured spatial distributions of spin polarization for drift along  $[110]$  and strain along  $[110]$  are shown in Fig. 3(a). The theoretical expectation [Fig. 3(b)] is obtained from the following considerations. Strain lifts the spin degeneracy and, like an “internal magnetic field” yields spin precession. In zinc blende type semiconductors, the spin precession angular frequency  $\Omega_p$  is given by [12, 19, 20, 21]

$$\Omega_{p,x} = \frac{C_3}{\hbar}(\epsilon_{xy}k_y - \epsilon_{xz}k_z) \text{ and cyclic permutations, (1)}$$

with the wave vector  $\mathbf{k}$  and the strain tensor  $\epsilon_{ij}$ . Another contribution including the diagonal elements of  $\epsilon_{ij}$  exists, but is negligibly small according to [12]. On the one hand, the statistical spin precession of thermalized electrons leads to spin relaxation as a contribution to the D'yakonov-Perel' (DP) mechanism. D'yakonov et al. [19] used the strain dependence of  $\tau_s$  to determine the constant  $C_3 = 5.2 \text{ eV}\text{\AA}$ . For drifting electrons, on the other hand, i.e. if the average wave vector is non-zero, the average electron spin will in general precess. For example if the drift is along  $[110]$  with velocity  $v_{\text{dr}}$ , i.e. with the

average wave vector  $\langle \mathbf{k} \rangle = v_{\text{dr}} m_e \hbar^{-1} \hat{\mathbf{e}}_{[110]}$ ,  $\hat{\mathbf{e}}_{[110]}$  being the unit vector along [110] and  $m_e$  the electron effective mass (0.067 $m_0$  for GaAs), and if the uniaxial strain is along [110] or [110] ( $\epsilon_{xy} = \epsilon_{yx} = \pm \epsilon_{[110],[1\bar{1}0]}/2 =: \epsilon/2$ , with all other off-diagonal elements vanishing) the average spin precession frequency vector, according to Eq. (1) will be  $\langle \Omega_p \rangle = \epsilon C_3 v_{\text{dr}} m_e \hbar^{-2} \hat{\mathbf{e}}_{[1\bar{1}0]}/2$ . Spin precession by  $2\pi$  of the electrons generated with initial orientation along [001] is expected at multiples of the precession period  $\Lambda_p = 2\pi v_{\text{dr}}/|\langle \Omega_p \rangle| = \frac{4\pi\hbar^2}{m_e \epsilon C_3} = 27.5 \text{ nm}/\epsilon$  (with  $C_3 = 5.2 \text{ eV\AA}$ ). Thus, the observed precession neither depends on the electric field nor on whether the strain is parallel or normal to the transport direction. From the linear fit in Fig. 3(c), we obtain  $\Lambda_p = 17.6 \text{ nm}/\epsilon$  or  $C_3 = 8.1 \text{ eV\AA}$ . Although the scatter of this data is low, we concede that the relatively coarse determination of  $\epsilon$  may lead to a systematic error of up to 30%, which is the largest uncertainty. The absence of spin precession for strain along [100] [c.f. Fig 3(d)] confirms that the influence of the diagonal elements of  $\epsilon_{ij}$  mentioned above is negligibly small.

We now focus on the influence of the drift field on electron spin relaxation. To our best knowledge realistic calculations of spin transport and its dependencies on the applied field, doping density, temperature and strain have not been reported before. Here we sketch the fundamentals of our theory and the most important numerical results, while details will be published elsewhere [9]. As Yu and Flatté [10] pointed out, electron spin transport can be treated in complete analogy to the ambipolar transport of electrons and holes (e.g. [11]), with the simplification that here “minority” and “majority” carriers have the same properties, except for their spin. Whereas the downstream and upstream diffusion lengths  $\Lambda_d$  and  $\Lambda_u$  exhibit a somewhat complicated field dependence, their difference turns out to be the spin drift length  $L_s$ , which is related to the spin lifetime by  $L_s = \Lambda_d - \Lambda_u = v_{\text{dr}} \tau_s$ . In the experiment, we determine  $\tau_s$  from this relation, while  $v_{\text{dr}}$  is obtained from the electron density, the sample geometry and the electric current. For low fields, both  $\Lambda_d$  and  $\Lambda_u$  converge to the spin diffusion length  $\Lambda_s = \sqrt{D_e \tau_s}$ ,  $D_e$  being the electron diffusion constant.

To calculate  $\tau_s$ , we basically follow the theory given in [12]. For the fields, temperatures and doping densities in our experiments, the DP [13] mechanism limited by ionized impurity scattering turns out to be the most important contribution. For this mechanism, the spin relaxation rate for an electron with energy  $E$  is given by  $\tilde{\tau}_s^{-1} = (32/105) \gamma_3^{-1} \tilde{\tau}_p \alpha_c^2 E^3 E_g^{-1} \hbar^{-2}$ . Here,  $\tilde{\tau}_p$  is the momentum relaxation time,  $E_g$  the band gap energy,  $\alpha_c \approx 0.063$ , and  $\gamma_3$  is a dimensionless parameter taking into account the scattering cross section. D'yakonov and Perel' argued that for small angle scattering (by ionized impurities)  $\gamma_3 \approx 6$ . However, a thorough analysis shows that this is only true for extremely small scattering

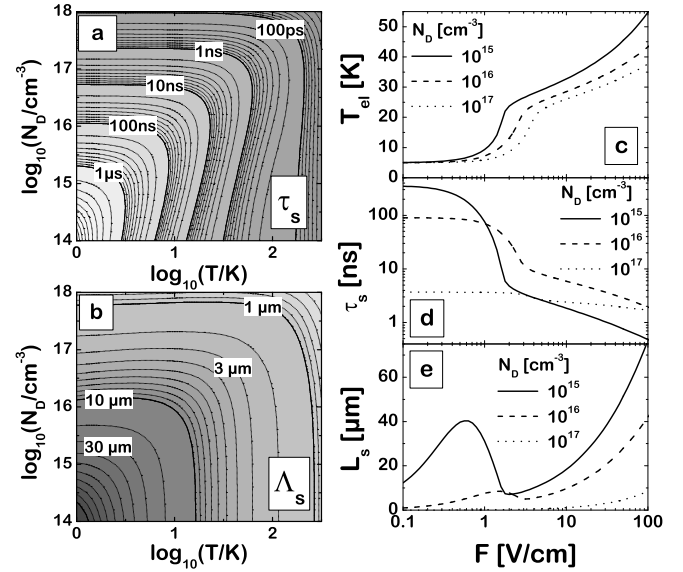


FIG. 4: (a): Calculated spin relaxation times ( $F = 0$ ); (b): calculated spin diffusion lengths ( $F = 0$ ); (c): expected field dependence of the electron temperature at  $T_L = 5 \text{ K}$ ; (d): resulting spin lifetimes, (e): resulting spin drift lengths.

angles. We therefore evaluate the parameter  $\gamma_3$  numerically, using the scattering cross section introduced by Ridley [14], which reduces  $\tau_s$  significantly (up to factor 5), especially at low  $T_L$  and  $N_D$ .

The total spin relaxation rate  $\tau_s^{-1}$  is obtained from the ensemble average of  $(\sum \tilde{\tau}_s)^{-1}$ , where the sum is over all scattering processes. This average has previously been taken either over a non-degenerate Boltzmann distribution (e.g. [13]) or has been evaluated at the Fermi energy for a strongly degenerate electron gas (e.g. [16]). By using a Fermi distribution, we cover both limiting cases and the intermediate regime. Taking into account also scattering by acoustic phonons (deformation potential and piezoelectric) and polar optical phonons, we obtain the spin relaxation times and the spin diffusion lengths at  $F = 0$  shown in Figs. 4(a) and (b), respectively. The calculated spin relaxation times reproduce well the measured values [15, 16] for delocalized electrons. However, as was pointed out by Kavokin [17] and Dzhioev et al. [16], this rate will not be correct for donor-bound electrons, i.e. at low temperatures and doping densities. Surprisingly, the measured low temperature ( $T_L = 4.2 \text{ K}$ ) spin lifetimes for  $2 \times 10^{15} \text{ cm}^{-3} < N_D < 2 \times 10^{16} \text{ cm}^{-3}$ , i.e. the range which is interpreted in terms of the anisotropic exchange interaction in [16], can also be explained by the DP mechanism in our calculations.

In the presence of an applied electric field  $F$ , the electron temperature  $T_{\text{el}}$  rises with respect to the lattice temperature  $T_L$  (e.g. [18]):

$$T_{\text{el}} = T_L + \frac{2e}{3k_B} v_{\text{dr}} F \frac{\langle E \rangle}{\langle E/\tau_E(E) \rangle}. \quad (2)$$

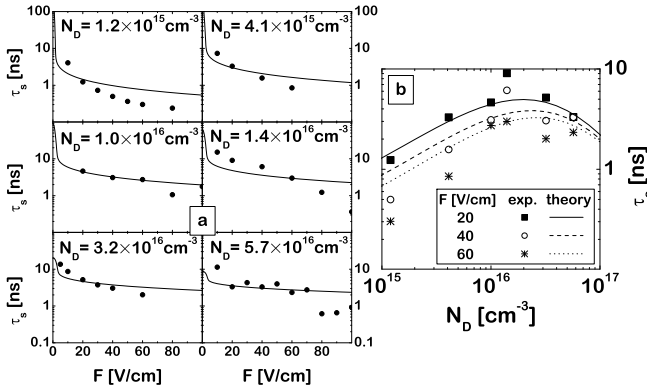


FIG. 5: (a) Field dependence of the measured and calculated spin lifetimes  $\tau_s$  at  $T_L = 5 \text{ K}$  and different doping densities  $N_D$ ; (b) doping density dependence at  $F = 20, 40, 60 \text{ V/cm}$ .

The angular brackets denote the averaging over the thermal distribution, and  $\tau_E(E)$  is the energy relaxation rate. Hence,  $T_{\text{el}}$ ,  $v_{\text{dr}}$ ,  $\tau_s$  and  $L_s$ , can be calculated self-consistently for a given lattice temperature, doping density and electric field from the energy and momentum relaxation rates. Figs. 4(c–e) show the expected dependencies of  $T_{\text{el}}$ ,  $\tau_s$  and  $L_s$  on the electric field for several doping densities at  $T_L = 5 \text{ K}$ . The steep increase of the electron temperature at low  $F$  to values of  $T_{\text{el}} \approx 30 \text{ K}$  can be attributed to the fact that all scattering mechanisms at very low electron temperatures are (quasi-)elastic and therefore inefficient energy relaxation mechanisms. Only at an increased electron temperature can the emission of optical phonons prevent a further increase of  $T_{\text{el}}$ . This strong increase of  $T_{\text{el}}$  is also reflected in  $\tau_s$  and consequently in  $L_s$  (approximately:  $\tau_s^{-1} \propto T_{\text{el}}^3$ ).

The field dependencies of the spin lifetimes at  $T_L = 5 \text{ K}$ , extracted from measurements like the one shown in Fig. 1(d) are plotted in Fig. 5(a) together with the theoretical expectation, while the doping density dependence can be seen in Fig. 5(b). Over the whole range of doping densities experiment and theory agree well at low fields. At all doping densities, however, the experimental values decrease faster with increasing electric field than expected, which may be due to sample heating by the electric current. Both our own measurements and the field dependence of  $\tau_s$  at low temperatures reported in [7] for  $N_D = 3 \times 10^{16} \text{ cm}^{-3}$  suggest that our calculations overestimate the increase of  $T_{\text{el}}$  at small fields.

Despite the stronger field dependence, the measured dependence of  $\tau_s$  on uniaxial strain along [110] and drift along [110] for  $N_D = 1.4 \times 10^{16} \text{ cm}^{-3}$ , shown in Fig. 6(a), agrees qualitatively with the theoretical expectation (b).

In conclusion, we have shown that spatially resolved Faraday rotation provides a sensitive tool to investigate spin relaxation and spin precession. We have attributed the observed strong decrease of the spin lifetimes at only small electric fields to the increased electron temperature.

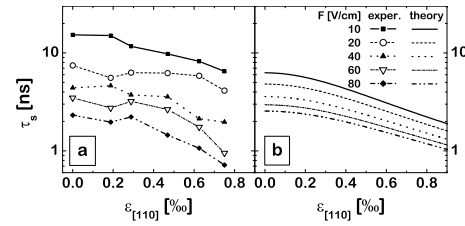


FIG. 6: Measured (a) and calculated (b) strain dependence of the spin lifetime at different electric fields [same sample and geometry as in Fig. 3(a)].

The possibility to apply tunable uniaxial strain allowed us to demonstrate the linear relation between the inverse spin precession length and the strain applied along the [110]-directions, as well as the absence of spin precession for strain along the [100]-directions. Thus, we were able to prove unambiguously that the zero magnetic field spin precession is a consequence of the strain-induced spin splitting first mentioned in [21] and to deduce the relevant band structure parameter  $C_3 = 8.1 \pm 2.5 \text{ eV}\text{\AA}$ .

- [1] I. Žutić, J. Fabian, and S. Das Sarma, Rev. Mod. Phys. **76**, 323 (2004).
- [2] R. R. Parsons, Phys. Rev. Lett. **23**, 1152 (1969).
- [3] A. P. Heberle, W. W. Rühle, and K. Ploog, Phys. Rev. Lett. **72**, 3887 (1994).
- [4] J. J. Baumberg *et al.*, Phys. Rev. Lett. **72**, 717 (1994).
- [5] J. M. Kikkawa and D. D. Awschalom, Nature **397**, 139 (1999).
- [6] Y. Kato *et al.*, Nature **427**, 50 (2004).
- [7] Y. Kato *et al.*, Phys. Rev. Lett. **93**, 176601 (2004).
- [8] S. A. Crooker and D. L. Smith, cond-mat/0411461 (2004).
- [9] M. Beck, in *Physik Mikrostrukturierter Halbleiter*, edited by S. Malzer, T. Marek and P. Kiesel (Lehrstuhl für Mikrocharakterisierung, Erlangen, 2005), Vol. 40, ISBN: 3-932392-57-3; M. Beck *et al.*, manuscript in preparation.
- [10] Z. G. Yu and M. E. Flatté, Phys. Rev. B **66**, 201202(R) and 235302 (2002).
- [11] R. A. Smith, *Semiconductors* (Cambridge University Press, London, New York, 1959).
- [12] G. E. Pikus and A. N. Titkov, in *Optical Orientation*, edited by F. Meier and B. P. Zakharchenya, (North-Holland, Amsterdam, 1984).
- [13] M. I. D'yakonov and V. I. Perel', Fiz. Tverd. Tela **13**, 3581 (1971); Sov. Phys. – Solid State **13**, 3023 (1972).
- [14] B. K. Ridley, J. Phys. C **10**, 1589 (1977).
- [15] J. M. Kikkawa and D. D. Awschalom, Phys. Rev. Lett. **80**, 4313 (1998).
- [16] R. I. Dzhioev *et al.*, Phys. Rev. B **66**, 245204 (2002).
- [17] K. V. Kavokin, Phys. Rev. B **64**, 075305 (2001).
- [18] M. Lundstrom, *Fundamentals of carrier transport*, edited by G. W. Neudeck and F. P. Pierret, Modular series on solid state devices Vol. 10 (Addison-Wesley, 1990).
- [19] M. I. D'yakonov *et al.*, *Thesis Union Conf. on the Physics of Semiconductors* (ELM, Baku, 1982), p. 146.

- [20] G. E. Pikus, V. A. Marushchak, and A. N. Titkov, Sov. Phys. Semicond. **22**, 115 (1988).
- [21] G. L. Bir and G. E. Pikus, Sov. Phys. – Solid State **3**, 2221 (1962).